



OPEN

Titanium dioxide particles frequently present in face masks intended for general use require regulatory control

Eveline Verleysen¹, Marina Ledecq¹, Lisa Siciliani¹, Karlien Cheyns², Christiane Vleminckx³, Marie-Noelle Blaude³, Sandra De Vos¹, Frédéric Brassinne¹, Frederic Van Steen¹, Régis Nkenda², Ronny Machiels², Nadia Waegeneers^{2,3}, Joris Van Loco^{1,2,3} & Jan Mast^{1,2}✉

Although titanium dioxide (TiO₂) is a suspected human carcinogen when inhaled, fiber-grade TiO₂ (nano)particles were demonstrated in synthetic textile fibers of face masks intended for the general public. STEM-EDX analysis on sections of a variety of single use and reusable face masks visualized agglomerated near-spherical TiO₂ particles in non-woven fabrics, polyester, polyamide and bi-component fibers. Median sizes of constituent particles ranged from 89 to 184 nm, implying an important fraction of nano-sized particles (<100 nm). The total TiO₂ mass determined by ICP-OES ranged from 791 to 152,345 µg per mask. The estimated TiO₂ mass at the fiber surface ranged from 17 to 4394 µg, and systematically exceeded the acceptable exposure level to TiO₂ by inhalation (3.6 µg), determined based on a scenario where face masks are worn intensively. No assumptions were made about the likelihood of the release of TiO₂ particles itself, since direct measurement of release and inhalation uptake when face masks are worn could not be assessed. The importance of wearing face masks against COVID-19 is unquestionable. Even so, these results urge for in depth research of (nano) technology applications in textiles to avoid possible future consequences caused by a poorly regulated use and to implement regulatory standards phasing out or limiting the amount of TiO₂ particles, following the safe-by-design principle.

Wearing face masks is an important and widely applied public health measure to control the COVID-19 pandemic¹. A recent study, testing several batches of face masks intended to be put on sale as personal protective equipment, showed that 70% of the examined face masks contained TiO₂ in quantities ranging from 100 to 2000 mg kg⁻¹². This suggests that TiO₂ is commonly applied in textiles of face masks, as in a wide variety of other textiles, e.g. to improve stability to ultraviolet light, as white colorant or as a matting agent^{3,4}. In addition, to introduce new solutions to the challenges associated with the COVID-19 pandemic, textile companies are incorporating specific nanofiber, nanocomposite and nanoparticle technology into face masks^{5,6}. Nanofibers containing TiO₂ nanoparticles have been produced to create antimicrobial filters⁷, also in combination with silver⁸ and graphene⁹. Coatings of TiO₂ nanoparticles on cotton fabric were applied for enhanced self-cleaning and antibacterial properties¹⁰.

In their recent opinion paper, Palmeiri et al.⁵ warn for the possible future consequences caused by a poorly regulated use of nanotechnology in textiles applied to improve the performance of face masks. In animal experiments, toxic effects were reported when TiO₂ particles were inhaled^{11,12}, as well as when they were ingested orally^{13,14}. In 2017, the Risk Assessment Committee (RAC) of the European Chemical Agency (ECHA) reviewed the carcinogenic potential of TiO₂ and proposed to classify Titanium dioxide as Carc. 2, H351 (suspected human carcinogen)¹⁵ by inhalation. This CLP classification¹⁶ was adopted for titanium dioxide.

To evaluate whether the TiO₂ particles in face masks possibly present a health risk, their amounts, their physicochemical properties and their localization were analyzed in a selection of face masks. Supporting on these measurements, the amount of TiO₂ at the surface of the textile fibers was estimated and compared with the acceptable exposure level to TiO₂ by inhalation, expressed per mask (AEL_{mask}).

¹Trace Elements and Nanomaterials, Sciensano, Groeselenbergstraat 99, 1180 Uccle, Belgium. ²Trace Elements and Nanomaterials, Sciensano, Leuvensesteenweg 17, 3080 Tervuren, Belgium. ³Service Risk and Health Impact Assessment, Sciensano, Juliette Wytsmanstraat 14, 1050 Brussels, Belgium. ✉email: jan.mast@sciensano.be

Results and discussion

Twelve face masks meant to be worn by the general population and including both single-use (disposable) and re-usable masks were obtained from various suppliers in Belgium and the EU. The origin of the masks is worldwide. The selected masks consist of a variety of fibers, including synthetic fibers, such as polyester, polyamide and meltblown and thermobonded non-woven fabrics; and natural fibers, such as cotton (Table 1). All masks are NIOSH uncertified, Mask04 and Mask07 have a CE logo; Mask03 and Mask07 are OEKO-TEX certified. Mask01, 04 and 05 are three ply type masks^{17,18}. Images of the examined masks are given as Supplementary Information 1.

Measurement of the total amount of titanium (Ti) in each face mask, as a proxy for the amount of TiO₂ particles, by inductively coupled plasma-optical emission spectroscopy (ICP-OES) showed that the amount of TiO₂ varied strongly, from 0.8 to 152 mg per mask (Table 1).

High angle annular dark field (HAADF)-scanning transmission electron microscopic (STEM) analysis of sections of the resin embedded face masks showed single and agglomerated constituent particles in synthetic fibers (Fig. 1a–c,e). The particles were observed in at least one layer of each examined face mask (Table 1 and Supplementary Information 2). Energy dispersive X-ray spectroscopy (EDX) analysis confirmed that these particles consist of TiO₂ (Fig. 2 and Supplementary Information 3). A fraction of the TiO₂ particles was located at the surface of the fibers (Fig. 2b). TiO₂ particles were not observed in cotton fibers (Fig. 1d), in meltblown non-woven fabrics (Fig. 1f), and in some of the thermobonded non-woven fabrics (Table 1).

In general, the electron microscopy results confirm the ICP-OES measurements showing that the amount of TiO₂ particles was approximately a factor 10 lower in non-woven fabrics than in polyester and polyamide fibers.

Measurements of the size and shape (near-spherical morphology) of the constituent TiO₂ particles and agglomerates in the examined face masks (Table 1, Supplementary Information 4–6) show that, overall, the physicochemical properties of the TiO₂ particles in face masks are in agreement with the specifications of so-called fiber-grade TiO₂ applied in other textiles^{19,20} and are similar to those of the E 171 food additive¹⁴. Although the measured TiO₂ size distributions in the face masks do not all qualify the applied TiO₂ as nanomaterials according to the EC-definition²¹, each examined mask, besides Mask04, contained a notable fraction of nanoparticles (6% to 65%), requesting an appropriate risk analysis.

Because the hazard of inhaled TiO₂ particles is well documented^{11,22,23}, particularly exposure analysis is important for risk analysis. Exposure to TiO₂ (nano)particles in face masks, depends on their level of release. Migration of agglomerated TiO₂ particles completely incorporated in the fiber polymers of face masks can be excluded by theoretical considerations: only particles smaller than 5 nm can migrate in the polymers constituting the face masks²⁴. Particles at the fiber surface might, however, be released when they are subjected to abrasion or to aerodynamic forces. Direct measurement of released particles is problematic because, to our knowledge, no standardized methods are available to determine whether particles are released from face masks during normal use, and which amount of TiO₂ is released. It is unknown if particles could be released as single particles, as agglomerates, as pieces of textile fibers containing agglomerates or a combination thereof, altering their fate. Moreover, few literature data are available that provide information on desorption/erosion/abrasion of TiO₂ particles from TiO₂-containing fibers²⁵. Therefore, an indirect approach was applied comparing the mass of TiO₂ at the surface of the textile fibers of each mask with the mass of TiO₂ particles that can be inhaled without adverse effects, expressed per mask (AEL_{mask}). This approach does not assume release of all particles at the fiber surface. It merely calculates which fraction of TiO₂ particles at the fiber surface has to be released to exceed the acceptable exposure level. Because the fate and release mechanisms of particles from face masks are currently unknown, no assumptions were made about the likelihood of the release of particles itself.

AEL_{mask} was estimated to be 3.6 µg using a threshold-based risk characterization for subchronic exposure with an intensive use scenario of face masks by the general adult population as described in Supplementary information 7. Lung inflammation was chosen as critical effect. A no observed adverse effect concentration of 0.5 mg/m³ was determined based on the repeated dose inhalation study with rats of Bermudez et al.¹² The risk was further characterized supporting on the approach to determine the professional acceptable exposure levels to TiO₂ nanoforms²⁶. The intensive use scenario assumed that 2 masks are worn over an 8-h period, with a recommended change of the masks every 4 h²⁷.

Furthermore, it was assumed that TiO₂ particles in the fiber matrix do not migrate and that only particles at the fiber surface can be released. The fraction (%) and the mass (µg) of TiO₂ particles at the fiber surface, were modelled assuming a homogenous particle distribution in the fibers as described in the methods section and Supplementary Information 9. This assumption is plausible because the TiO₂ particles are mixed with the fiber matrix during production and was confirmed by HAADF-STEM analysis. For typical (near-)cylindrical synthetic fibers (polyester, polyamide and non-woven), percentages ranged from 2 to 4%. Estimated amounts of TiO₂ at the fiber surface per mask ranged from 17 to 4394 µg (Table 1). Because the structure of bi-component microfibers (Fig. 1c) results in a larger surface area²⁸, a correction factor was introduced resulting in higher percentages of particles at the surface (in the methods section and Supplementary Information 9).

Table 1 shows that for all examined face masks, the amount of TiO₂ particles at the surface of the textile fibers notably exceeds the AEL_{mask}. This systematic exceedance indicates that by applying an approach relying on conservative assumptions while uncertainties regarding hazard and exposure remain (Supplementary Information 7), a health risk cannot be ruled out when face masks containing polyester, polyamide, thermobonded non-woven and bi-component fibers, are used intensively. Exceedance of the AEL_{mask} for reusable face masks is higher (87 to 1220 times) than for single use masks (5 to 11 times), implying that for the reusable masks uptake of only a very small percentage of the particles at the fiber surface may already pose a health risk. Reusable masks typically have higher TiO₂ amounts in the matrix, have a higher mass (more textile corresponds with more TiO₂), and have smaller mean fiber diameters than single use masks. For all examined masks, the combined measurement uncertainty (k = 1) on the total mass of TiO₂ (Table 1, Supplementary Information 8) was larger than AEL_{mask}.

Ref	Type ^a	Layers	Composition ^a	Fiber diameter ^b (μm)	AA size ^c (nm)	CP size ^d (nm)	Modelled fraction of TiO ₂ on fiber surface (%)	Total TiO ₂ per mask ^f (μg)	Estimated amount of TiO ₂ at fiber surface per mask (μg)	Times the amount of TiO ₂ at fiber surface exceeds AEL _{mask}
Mask01	Single-use	External	Thermobonded non-woven ^e	24 ± 7.4	197 ± 59	131 ± 61	2	2386 ± 286	39	11
		Central	Meltblown non-woven	–	–	–	–			
		Internal	Thermobonded non-woven	–	–	–	–			
Mask02	Reusable	External	Polyester ^e	9 ± 0.7	123 ± 76	125 ± 72	3	17,332 ± 2080	462	128
		Central	Meltblown non-woven	–	–	–	–			
		Internal	100% cotton	–	–	–	–			
Mask03	Reusable	External	100% polyester ^e	9 ± 0.9	188 ± 121	124 ± 48	4	30,757 ± 3691	1056	293
		Central	65% polyester, 35% cotton ^e	11 ± 0.7	156 ± 104	107 ± 59	3			
		Internal	65% polyester, 35% cotton ^e	11 ± 2.0	173 ± 101	133 ± 45	3			
Mask04	Single-use	External	Thermobonded non-woven ^e	21 ± 1.8	220 ± 66	182 ± 80	2	1370 ± 164	30	8
		Central	Meltblown non-woven	–	–	–	–			
		Internal	Thermobonded non-woven ^e	23 ± 7.2	274 ± 76	143 ± 97	2			
Mask05	Single-use	External	Thermobonded non-woven ^e	19 ± 2.5	233 ± 107	184 ± 74	2	791 ± 95	17	5
		Central	Meltblown non-woven	–	–	–	–			
		Internal	Thermobonded non-woven ^e	18 ± 2.8	171 ± 82	168 ± 58	2			
Mask06	Reusable	External	Polyester ^e	7 ± 0.4	147 ± 57	101 ± 46	4	12,195 ± 1463	448	87
		Central	Unknown ^e	35 ± 8.4	409 ± 182	117 ± 32	2			
		Internal	Cotton	–	–	–	–			
Mask07	Reusable	External	Polyamide ^e	9 ± 1.2	130 ± 98	96 ± 38	3	152,345 ± 18,281	4394	1220
		Internal	Polyamide ^e	9 ± 0.7	135 ± 118	103 ± 44	3			
Mask08	Reusable		Polyester, polyamide, elastane ^e	11 ± 1.0	184 ± 87	99 ± 50	3	9573 ± 1149	327	136
Mask09	Reusable	External	Thermobonded non-woven ^e	24 ± 6.5	450 ± 130	147 ± 73	4	2298 ± 276	84	16
		Central	Meltblown non-woven	–	–	–	–			
		Internal	Thermobonded non-woven ^e	23 ± 6.4	372 ± 177	157 ± 56	3			
Mask10	Reusable	External	Polyester ^e	11 ± 0.8	110 ± 84	90 ± 40	2	17,427 ± 2091	358	99
		Internal	Cotton	–	–	–	–			
Mask11	Reusable	External	Polyester ^e	10 ± 0.6	135 ± 69	89 ± 32	3	12,713 ± 1526	352	98
		Central	Thermobonded non-woven	–	–	–	–			
		Internal	Cotton	–	–	–	–			
Mask12	Reusable	External	Bi-component microfiber ^e	13 ± 0.8	173 ± 95	105 ± 45	8	12,929 ± 1552	1054	293
		Internal	Bi-component microfiber ^e	12 ± 1.7	191 ± 104	96 ± 43	9			

Table 1. Properties of the examined face masks. ^aAs indicated on the packaging or based on expert advice. ^bMedian ± interquartile range (IQR) of the fiber diameter. ^cMinimum external dimension of the TiO₂ agglomerates (AA) estimated as the median ± interquartile range (IQR) of the minimum Feret diameter distribution. ^dMinimum external dimension of the TiO₂ constituent particles (CP) estimated as the median ± IQR of the minimum Feret diameter distribution. ^eTiO₂ particles were observed in this layer by STEM-EDX. ^fThe combined measurement uncertainty ($k=1$) on the total mass of TiO₂ per mask was calculated based on an in-house validation study (see Supplementary Information 8). The uncertainty related to the weight of the mask is not included in this uncertainty.

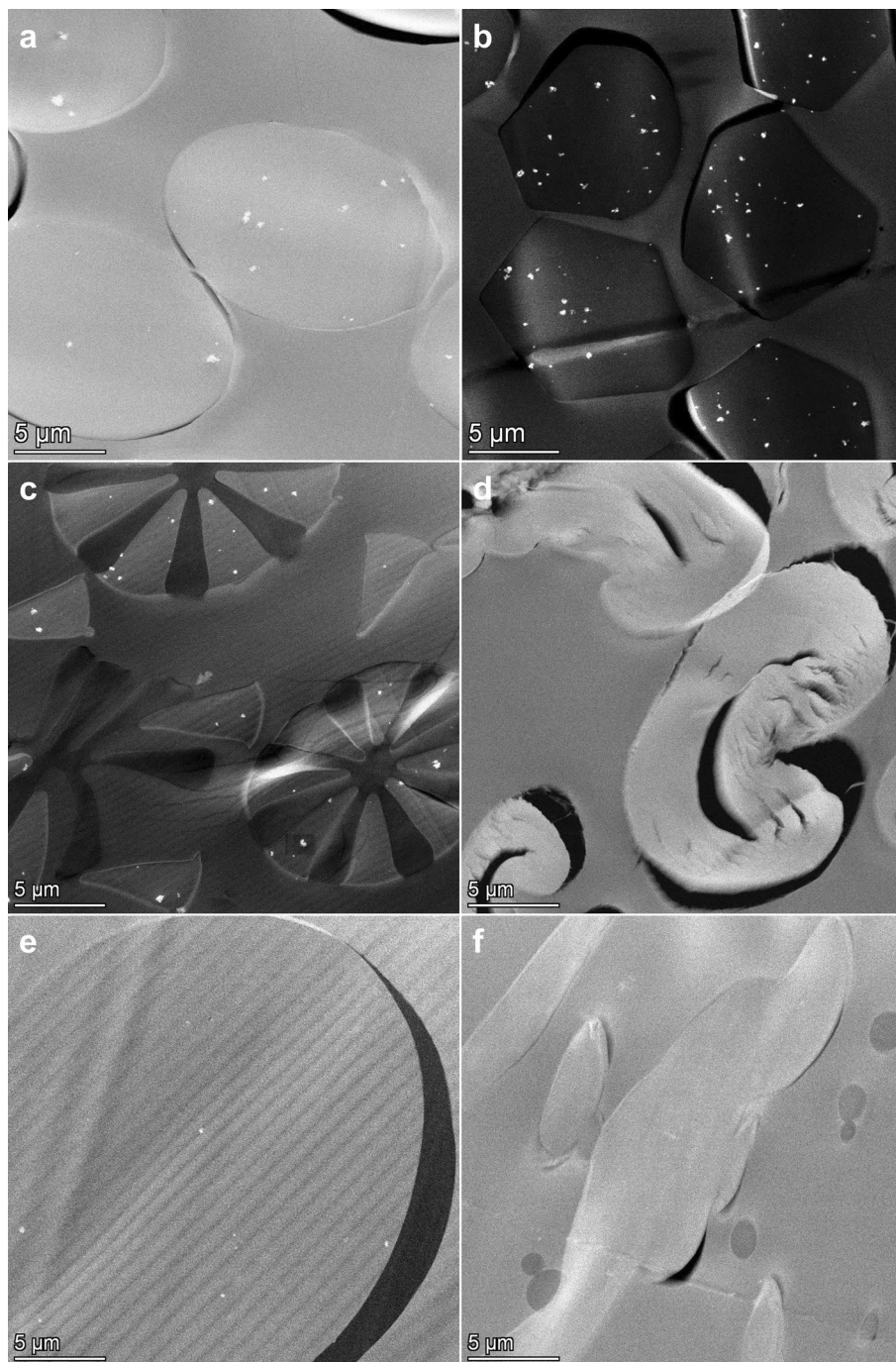


Figure 1. HAADF-STEM images of sections of different types of fibers observed in the face masks, with (a) polyester, (b) polyamide, (c) bi-component microfiber, (d) cotton, (e) thermobonded non-woven fiber, (f) meltblown non-woven fabric. TiO_2 particles are visible as bright white dots.

Consequently, TiO_2 release in the order of AEL_{mask} , measured as the change in TiO_2 before and after wearing the mask, cannot be demonstrated since it falls within the uncertainty range of the total mass measurement.

Face mask have an important role in the measures against the COVID-19 pandemic¹. So far, no data are available that indicate that the possible risk associated with the presence of TiO_2 particles in face masks outweighs the benefits of wearing face masks as protection measure. That is why we do not call for people to stop wearing face masks. However, the warning of Palmeiri et al.⁵ for the possible future consequences caused by a poorly regulated use of nanotechnology in textiles should be extended to face masks where TiO_2 particles are applied conventionally, as a white colorant or as a matting agent, or to assure durability reducing polymer breakdown by ultraviolet light^{3,4}. These properties are not critical for the functioning of face masks, and synthetic fibers suitable for face mask can be produced without TiO_2 ²⁹ as was observed in the layers of several masks (Table 1).

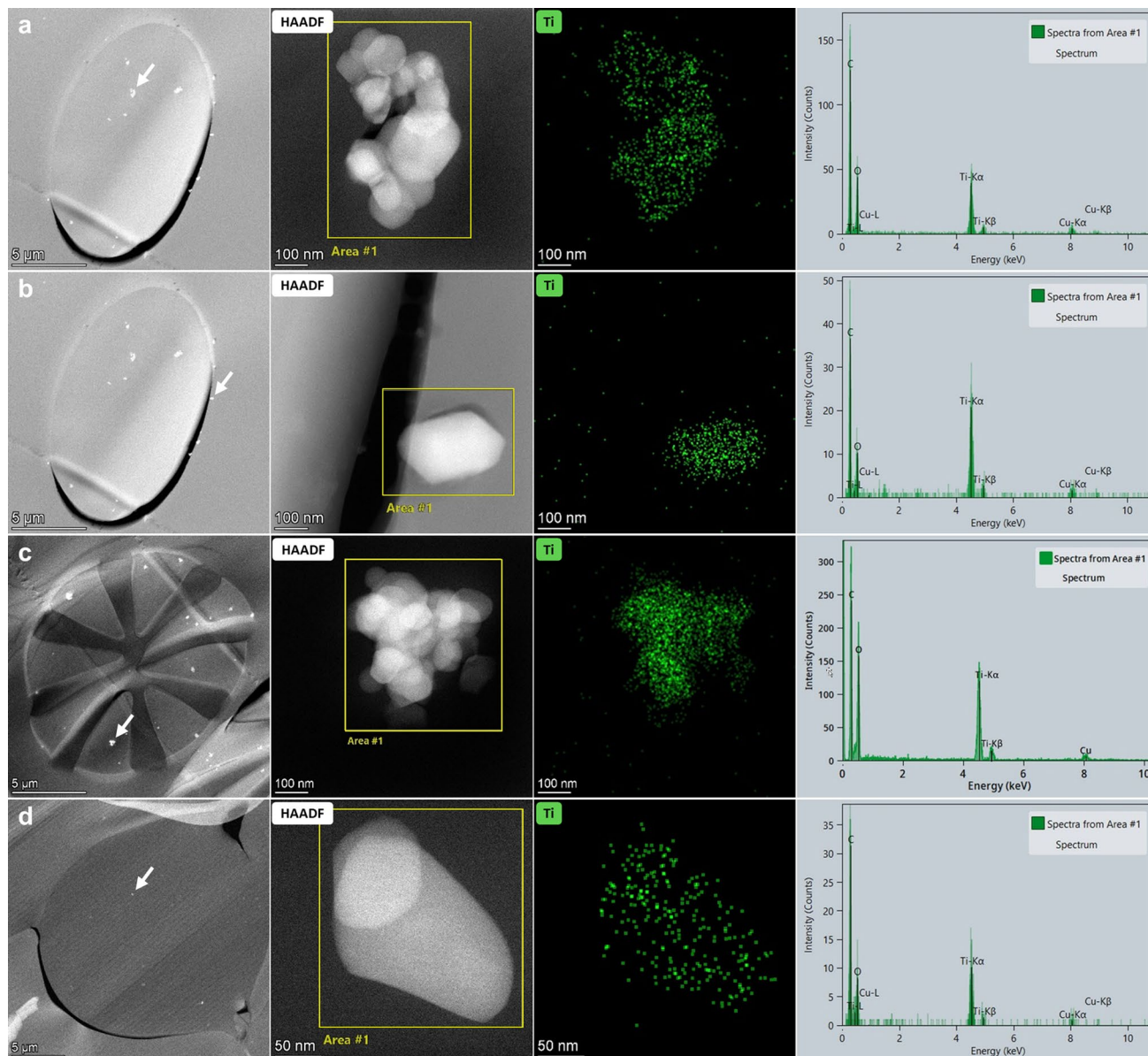


Figure 2. STEM-EDX analysis of particles (a) in a polyester fiber, (b) at the edge of a polyester fiber, (c) in a bi-component microfiber and (d) in a non-woven fabric. (first column) The low magnification HAADF-STEM images show the cross sections of the fibers containing the analyzed particles (white arrows) shown in the (second column) higher magnification HAADF-STEM images. (third column) The spectral images of Ti (green) obtained by EDX show that the measured Ti signal coincides with the position of the particles shown in the STEM image, and (fourth column) the EDX spectra of the area's indicated on the STEM image show the Ti signal.

Moreover, uncertainties regarding the genotoxicity of TiO_2 particles remain¹⁴. Therefore, these results urge for the implementation of regulatory standards phasing out or limiting the amount of TiO_2 particles, according to the 'safe-by-design' principle.

The applied approach allowed to assess one of the quality parameters of face masks quantitatively: the amount of TiO_2 at the fiber surface. Such quantitative parameter is important to evaluate the face masks present on the market, to develop product specifications and regulatory standards, and to produce better products.

In the course of this study, we identified several major challenges related to the analysis, characterization and risk assessment of TiO_2 in face masks, which go beyond the scope of the study: (i) In general, scientific data on the presence of (nano)particles in face masks, their characteristics, the exposure and the risks for the population is limited. (ii) Methodologies for characterizing TiO_2 particles in face masks are time consuming and expensive. (iii) Even though this study focused on face masks intended for the general public, this does not exclude TiO_2 from being present in other types of masks containing synthetic fibers, such as medical masks, even when they are certified. The presented study on face masks for the general population should be extended to assess the potential health risks associated with the presence of TiO_2 particles in medical and personal protection equipment face

masks and consequent occupational exposure. (iv) The fate and release mechanisms of particles from face masks are currently unknown, e.g. particles could be released as single particles, as agglomerates, as pieces of fibers containing agglomerates or a combination thereof. Agglomerates are sensitive to changes in the environment such as pH, ionic strength, presence of proteins and motion of the carrier medium, and can de-agglomerate or agglomerate further depending on the environment^{30,31}. While this induces complex behavior of nanoparticles in exposure scenarios and in tissue uptake and bio-distribution, influence on toxicity or biological responses remain poorly understood^{30,32}. (v) Key information about the toxicity of TiO₂ particles is missing for risk assessment: data about the hazard (inhalation toxicity threshold) of the specific TiO₂ particles present in face masks should be determined in a robust, repeated dose inhalation study with fiber-grade TiO₂ particles. Furthermore, more toxicity and epidemiological research is needed to assess the risk of vulnerable populations, especially children.

Methods

ICP-OES sample preparation. The examined face masks consisted of materials that are very resistant to the digestion steps typically applied to prepare samples for total titanium (Ti) analysis by ICP-OES. Adaptation of the sample preparation method based on closed-microwave assisted acid digestion allowed, however, measuring the total amount of Ti. The masks were homogenized by cutting them into small pieces using scissors and mixing the cuts manually. When the masks contained both woven and non-woven textile layers, the layers were digested separately. When the masks contained non-woven textile layers only, making their separation difficult, the entire mask was homogenized.

Two digestion methods were applied, depending on the material. Woven textiles (cotton, polyester or other synthetic fibers) were digested (closed microwave digestion) in a 4:1 (v:v) mixture of nitric acid and sulfuric acid at 220 °C in a Mars 6 microwave (CEM, USA). This method was adapted from the application note for polyethylene terephthalate digestion³³. The non-woven textiles from the masks needed higher temperatures for complete digestion, and the method was adapted to the light fibers that were not easily wetted. The method uses first a charring step in concentrated sulfuric acid at 260 °C in iPrep vessels (CEM, USA), followed by a digestion step in concentrated nitric acid at 200 °C.

ICP-OES analysis. After dilution of the digests, the total Ti concentration was determined by ICP-OES at wavelength 368.520 nm (Varian 720, Agilent technologies). All samples were prepared and analyzed in duplicate. Titanium concentrations were recalculated to TiO₂ concentrations by multiplying them with a factor 1.668, calculated as the ratio of the molecular mass of TiO₂ (79.88 g/mol) to that of Ti (47.88 g/mol), assuming all Ti is present as TiO₂.

TEM sample preparation. A sample preparation methodology for TEM analysis of particles in textiles was developed based on Gashti et al.³⁴, Lorenz et al.³⁵, Hebeish et al.³⁶ and Joshi et al.³⁷.

From each mask, a 1 × 1 cm square piece was cut using scissors, and the different layers of the mask were separated. From each layer, a 1 × 5 mm strip was cut. Each strip was transferred into a silicone rubber embedding mold [Silicone Mould 21 Cavity Blue (Agar Scientific Ltd., G3549)] and embedded in EPON812-Spurr resin mixture.

Specimen blocks were trimmed using a TM60 trimming unit (Reichert-Jung A.G., Vienna, Austria) to obtain a cutting face of 0.5–2 mm². Semi-thin sections with a section thickness between 150 and 250 nm were cut using the an Ultracut ultramicrotome (Leica Microsystems, Wetzlar, Germany). The sections were brought on carbon and pioloform-coated 150 mesh copper grids (Agar Scientific Ltd., G2150C; carbon and pioloform layers were added in-house).

TEM imaging and analysis. Sections of face masks were analyzed using a Talos F200S G2 transmission electron microscope equipped with an HAADF detector and Super-X EDS detector (Thermo Fisher Scientific, Eindhoven, The Netherlands) consisting of 2 windowless silicon drift detectors (SDD) (Thermo Fisher Scientific, Eindhoven, The Netherlands). STEM imaging, aiming to detect, localize and measure the size, morphology and agglomeration state of TiO₂ particles, and EDX spectra and spectral images, aiming to determine the elemental composition of the observed particles, were recorded using the Velox software (Thermo Fisher Scientific). Descriptive analyses, including elemental analyses, were done in triplicate, based on three individual masks. The size distributions of the constituent particles and of the agglomerates of TiO₂ particles were estimated by recording ten representative images at high and low magnification, respectively, followed by image analysis using the ImageJ software^{38–40}. The magnification selected for quantitative analysis of agglomerates was selected based on the size of the cross sections of the fibers, and was layer dependent. Agglomerate size was determined semi-automatically using the Particlesizer plugin in single particle mode. For quantitative analysis of constituent particles, a magnification of 88,000 times was selected in all cases. Dispersion methods, as applied for the characterization of constituent particles in the E171 food additive^{41,42} and needed to separate the particles from the matrix and for precise subsequent (semi-automatic) image analysis, cannot be applied for the particles in the face masks, which are embedded as agglomerates in a polymer matrix. Therefore, measurement of constituent particles relied on manual measurement of limited datasets, which is relatively imprecise and explains also part of the observed variation in size. The number of measured particles depended on the TiO₂ concentration in the fibers and ranged from 30 to 166 constituent particles and 12 to 416 agglomerates in ten images at the selected magnification. The raw data resulting from the image analyses was processed using an in-house Python script for calculation of descriptive statistics and for plotting histograms. The surface area of the cross-sections of the fibers was measured based on TEM images using the ImageJ software, and verified by light microscopy.

Estimation of the fraction of TiO₂ particles at the fiber surface. The mass of the (agglomerated) TiO₂ particles at the surface of the fibers in a mask (M_{sf}), can be calculated as:

$$M_{sf} = F * M_{tot} \quad (1)$$

with F the fraction of the particles at the surface of the fibers and M_{tot} the total mass of TiO₂ in the mask.

Assuming a homogeneous distribution of the agglomerated TiO₂ particles in the fibers, F is approximated as the ratio of an external ring-shaped surface of the cross-section of the fibers (S_r) and the total surface of the cross-section of the fibers (S_{cs}) (Supplementary Information 9). The thickness of the external ring-shaped surface, S_r , is determined by the median diameter (d_f) of the TiO₂ agglomerates (Supplementary Information 9). This can be approximated, assuming circular cross-sections of fibers, as:

$$F = \frac{S_r}{S_{CS}} \quad (2)$$

$$F = \frac{\frac{\pi}{4} * d_f^2 - \frac{\pi}{4} * (d_f - d_a)^2}{\frac{\pi}{4} * d_f^2} \quad (3)$$

$$F = \frac{d_f^2 - (d_f - d_a)^2}{d_f^2} \quad (4)$$

with d_f the median diameter of the fibers and d_a the median minimum Feret diameter of the TiO₂ agglomerates.

For a specific case of fibers, namely bi-component microfibers, the assumption of a homogeneous distribution of the agglomerated TiO₂ particles in the fibers is incorrect. Bi-component microfibers are characterized by a larger surface area from which TiO₂ particles can be released. To account for this increased surface, $S_{r,mf}$, a correction factor was introduced:

$$S_{r,mf} = S_r * \frac{\sum \text{wedges perimeter}}{\text{fiber perimeter}} \quad (5)$$

With $\sum \text{wedges perimeter}$ the sum of the perimeters of the wedge-shaped (TiO₂ containing) polyester parts of the fiber, and fiber perimeter the perimeter of the (near-)circular cross-section of the microfiber.

Data availability

The datasets generated during and/or analysed during the current study are available from the corresponding author on reasonable request.

Received: 25 November 2021; Accepted: 1 February 2022

Published online: 15 February 2022

References

1. Peeples, L. Face masks: What the data say. *Nature* **586**, 186–189 (2020).
2. Pedicini, P., D'Amato, R., Evi, E. & Corrao, I. Parliamentary question E-005899/2020 to European Parliament: Titanium dioxide in personal protective equipment (PPE).
3. Karbownik, I., Kowalczyk, D., Malinowska, G. & Paruch, B. Antibacterial properties of polyester fibres' materials with titanium dioxide deposited on their surface. in *Proc. III Natl. Conf. Nanotechnol. Acta Phys. Pol. A* (2009).
4. Gao, C. *et al.* Continuous dry-wet spinning of white, stretchable, and conductive fibers of poly(3-hydroxybutyrate-co-4-hydroxybutyrate) and ATO@TiO₂ nanoparticles for wearable e-textiles. *J. Mater. Chem. C* **8**, 8362–8367 (2020).
5. Palmieri, V., De Maio, F., De Spirito, M. & Papi, M. Face masks and nanotechnology: Keep the blue side up. *Nano Today* **37**, 101077 (2021).
6. Valdiglesias, V. & Laffon, B. The impact of nanotechnology in the current universal COVID-19 crisis: Let's not forget nanosafety!. *Nanotoxicology* **14**, 1013–1016 (2020).
7. Lee, B.-Y. *et al.* Titanium dioxide-coated nanofibers for advanced filters. *J. Nanoparticle Res.* **12**, 2511–2519 (2010).
8. Li, Y., Leung, P., Yao, L., Song, Q. W. & Newton, E. Antimicrobial effect of surgical masks coated with nanoparticles. *J. Hosp. Infect.* **62**, 58–63 (2006).
9. Bhattacharjee, S., Joshi, R., Chughtai, A. A. & Macintyre, C. R. Graphene modified multifunctional personal protective clothing. *Adv. Mater. Interfaces* **6**, 1900622 (2019).
10. Aalipourmohammadi, M., Davodiroknabadi, A. & Nazari, A. Homogeneous coatings of titanium dioxide nanoparticles on corona-treated cotton fabric for enhanced self-cleaning and antibacterial properties. *Autex Res. J.* **21**, 101–107 (2021).
11. National Institute for Occupational Safety and Health (NIOSH). *NIOSH Current Intelligence Bulletin 63: Occupational Exposure to Titanium Dioxide*.
12. Bermudez, E. *et al.* Pulmonary responses of mice, rats, and hamsters to subchronic inhalation of ultrafine titanium dioxide particles. *Toxicol. Sci.* **77**, 347–357 (2004).
13. Bettini, S. *et al.* Food-grade TiO₂ impairs intestinal and systemic immune homeostasis, initiates preneoplastic lesions and promotes aberrant crypt development in the rat colon. *Sci. Rep.* **7**, 40373 (2017).
14. EFSA Panel on Food Additives and Flavours (FAF). Safety assessment of titanium dioxide (E171) as a food additive. *EFSA J.* **19**, 1–10 (2021).
15. ECHA Committee for Risk Assessment (RAC). *Opinion Proposing Harmonised Classification and Labelling at EU Level of Titanium Dioxide*. <https://echa.europa.eu/documents/10162/682fac9f-5b01-86d3-2f70-3d40277a53c2> (2017).
16. European Commission. Commission Delegated Regulation (EU) 2020/217 of 4 October 2019 amending, for the purposes of its adaptation to technical and scientific progress, Regulation (EC) No 1272/2008 of the European Parliament and of the Council on

- classification, labelling and packaging of substances and mixtures and correcting that Regulation. *Off. J. Eur. Union*. Accessed 18 Feb 2020.
17. Neupane, B. B. & Giri, B. Review of materials and testing methods for virus filtering performance of face mask and respirator. *PeerJ Mater. Sci.* **3**, e17 (2021).
 18. Chua, M. H. *et al.* Face masks in the new COVID-19 normal: Materials, testing, and perspectives. *Research* **2020**, 1–40 (2020).
 19. Shanghai Liangjiang Titanium Chemical Co., Ltd. *Titanium Dioxide (Fiber Grade)*. <http://www.liangjiangchem.com/e25.htm>.
 20. Shanghai Zhongjing International Trade Co., Ltd. *Titanium Dioxide TiO₂ in Textile Industry*. <https://www.tidoxe.com/titanium-dioxide-in-fiber-grade.html>.
 21. EC. Commission recommendation of 18 October 2011 on the definition of nanomaterial. *Off. J. Eur. Union* **1**, 38–40 (2011).
 22. Lee, K. P., Trochimowicz, H. J. & Reinhardt, C. F. Pulmonary response of rats exposed to titanium dioxide (TiO₂) by inhalation for two years. *Toxicol. Appl. Pharmacol.* **79**, 179–192 (1985).
 23. Heinrich, U. *et al.* Chronic inhalation exposure of wistar rats and two different strains of mice to diesel engine exhaust, carbon black, and titanium dioxide. *Inhal. Toxicol.* **7**, 533–556 (1995).
 24. Franz, R., Bott, J. & Störmer, A. Considerations for and guidance to testing and evaluating migration/release of nanoparticles from polymer based nanocomposites. *Nanomaterials* **10**, 1113 (2020).
 25. Windler, L. *et al.* Release of titanium dioxide from textiles during washing. *Environ. Sci. Technol.* **46**, 8181–8188 (2012).
 26. ANSES. Valeurs limites d'exposition en milieu professionnel. Le dioxyde de titane sous forme nanométrique (TiO₂-NP, P25) Rapport d'expertise collective, Décembre 2020—Expertise scientifique. Saisine n° 2019-SA-0109—LEP TiO₂-NP. (2020).
 27. Coronavirus COVID-19 information website of the Belgian federal public service for Health. *Food Chain Safety and Environment*. <https://www.info-coronavirus.be/en/facemask/>.
 28. Hosseini Ravandi, S. A. & Valizadeh, M. Properties of fibers and fabrics that contribute to human comfort. in *Improving Comfort in Clothing* 61–78 (Elsevier, 2011). <https://doi.org/10.1533/9780857090645.1.61>.
 29. Militky, J. The chemistry, manufacture and tensile behaviour of polyester fibers. in *Handbook of Tensile Properties of Textile and Technical Fibres* 223–314 (Elsevier, 2009). <https://doi.org/10.1533/9781845696801.2.223>.
 30. Bruinink, A., Wang, J. & Wick, P. Effect of particle agglomeration in nanotoxicology. *Arch. Toxicol.* **89**, 659–675 (2015).
 31. Tourinho, P. S. *et al.* Metal-based nanoparticles in soil: Fate, behavior, and effects on soil invertebrates. *Environ. Toxicol. Chem.* **31**, 1679–1692 (2012).
 32. Mitrano, D. M., Motellier, S., Clavaguera, S. & Nowack, B. Review of nanomaterial aging and transformations through the life cycle of nano-enhanced products. *Environ. Int.* **77**, 132–147 (2015).
 33. CEM. *MARS 6TM Method Note Microwave Digestion of PET*.
 34. Gashti, M. P., Alimohammadi, F., Song, G. & Kiumarsi, A. Characterization of nanocomposite coatings on textiles: A brief review on microscopic technology. *Curr. Microsc. Contrib. Adv. Sci. Technol.* **2**, 1424–1437 (2012).
 35. Lorenz, C. *et al.* Characterization of silver release from commercially available functional (nano) textiles. *Chemosphere* **89**, 817–824 (2012).
 36. Hebeish, A. *et al.* Highly effective antibacterial textiles containing green synthesized silver nanoparticles. *Carbohydr. Polym.* **86**, 936–940 (2011).
 37. Joshi, M., Bhattacharyya, A. & Ali, S. W. *Characterization Techniques for Nanotechnology Applications in Textiles* (Springer, 2008).
 38. Rasband, W. S. *ImageJ*. <https://imagej.nih.gov/ij/> (1997).
 39. Schneider, C. A., Rasband, W. S. & Eliceiri, K. W. NIH Image to ImageJ: 25 years of image analysis. *Nat. Methods* **9**, 671–675 (2012).
 40. Abramoff, M. D., Magalhaes, P. J. & Ram, S. J. Image processing with ImageJ. *Biophoton. Int.* **11**, 36–42 (2004).
 41. Verleysen, E. *et al.* Towards a generic protocol for measuring the constituent particle size distribution of E171 in food by electron microscopy. *Food Control* **132**, 108492 (2022).
 42. Verleysen, E. *et al.* Physicochemical characterization of the pristine E171 food additive by standardized and validated methods. *Nanomaterials* **10**, 592 (2020).

Acknowledgements

This work is part of a COVID-19 project funded by the federal government of Belgium. The authors would like to thank Mirjana Andjelkovic for contributing to scientific discussions.

Author contributions

Conceptualization, J.M., E.V., K.C., C.V., M.-N.B., J.V.L.; methodology, E.V., M.L., K.C., N.W., J.M., M.-N.B., C.V.; formal analysis, L.S., M.L., E.V., S.D.V., F.B., F.V.S., K.C., R.N., R.M., M.-N.B.; data curation, J.M., E.V., L.S., K.C., M.-N.B.; writing—original draft preparation, E.V., J.M., K.C., L.S.; writing—review and editing, E.V., J.M., K.C., M.-N.B., C.V., J.V.L., N.W.; visualization, E.V., L.S.; supervision J.M., J.V.L., E.V., K.C., C.V.; project administration, J.M., E.V.; funding acquisition J.M., J.V.L., E.V. All authors have read and agreed to the published version of the manuscript.

Competing interests

The authors declare no competing interests.

Additional information

Supplementary Information The online version contains supplementary material available at <https://doi.org/10.1038/s41598-022-06605-w>.

Correspondence and requests for materials should be addressed to J.M.

Reprints and permissions information is available at www.nature.com/reprints.

Publisher's note Springer Nature remains neutral with regard to jurisdictional claims in published maps and institutional affiliations.



Open Access This article is licensed under a Creative Commons Attribution 4.0 International License, which permits use, sharing, adaptation, distribution and reproduction in any medium or format, as long as you give appropriate credit to the original author(s) and the source, provide a link to the Creative Commons licence, and indicate if changes were made. The images or other third party material in this article are included in the article's Creative Commons licence, unless indicated otherwise in a credit line to the material. If material is not included in the article's Creative Commons licence and your intended use is not permitted by statutory regulation or exceeds the permitted use, you will need to obtain permission directly from the copyright holder. To view a copy of this licence, visit <http://creativecommons.org/licenses/by/4.0/>.

© The Author(s) 2022